CONF-9506256--2

LA-UR- 95-2888

Title: ULYSSES SOLAR WIND PLASMA OBSERVATIONS FROM PEAK SOUTHERLY LATITUDE THROUGH PERIHELION AND BEYOND

Author(s):
J. L. Phillips
S. J. Bame
W. C. Feldman
J. T. Gosling
D. J. McComas
B. E. Goldstein
M. Neugebauer
C. M. Hammond

Submitted to: Proceedings of the Eighth International Solar Wind Conference

Los Alamos
NATIONAL LABORATORY

Form No. 836 R5
ST 2629 10/91

Ulysses Solar Wind Plasma Observations from Peak Southerly Latitude Through Perihelion and Beyond

J.L. Phillips, S.J. Bame, W.C. Feldman, J.T. Gosling, and D.J. McComas
Los Alamos National Laboratory

B.E. Goldstein and M. Neugebauer
Jet Propulsion Laboratory

C.M. Hammond
SRI International

Abstract. We present Ulysses solar wind plasma data from the peak southerly latitude of -80.2° through +64.9° latitude on June 7, 1995. Ulysses encountered fast wind throughout this time except for a 43° band centered on the solar equator. Median mass flux was nearly constant with latitude, while speed and density had positive and negative poleward gradients, respectively. Solar wind momentum flux was highest at high latitudes, suggesting a latitudinal asymmetry in the heliopause cross section. Solar wind energy flux density was also highest at high latitudes.

INTRODUCTION

The solar wind plasma experiment on Ulysses measured the solar wind throughout the southern solar hemisphere and into the northern hemisphere using separate ion and electron spectrometers [*Bame et al.*, 1992]. After southward deflection at Jupiter in February 1992, the spacecraft initially encountered slow and irregular solar wind. As Ulysses passed -13° latitude in July 1992, it entered a recurrent pattern of alternating high speed wind from the south polar coronal hole and slower equatorial wind [*Bame et al.*, 1993]. This pattern repeated every ~26 days through early July 1993, when the spacecraft emerged into continuous fast wind. Fast wind continued through the peak southerly latitude of -80.2° at 2.29 AU on 13 September 1994 [*Phillips et al.*, 1995*a*]. At

low and mid latitudes numerous corotating interaction regions (CIRs) were observed, with flow deflections and a shock pattern indicating that solar rotation and the tilt of the solar magnetic dipole caused systematic equatorward (poleward) propagation of the forward (reverse) shocks bounding the CIRs [*Gosling et al.*, 1993; *Pizzo and Gosling*, 1994]. Coronal mass ejections were observed through -60.5°, with three events having forward-reverse shock pairs caused, not by a speed differential, but by expansion of the ejecta [*Gosling et al.*, 1994]. The high-latitude wind was structured by Alfvénic, compressional, and pressure-balanced features, the latter possibly being the interplanetary manifestations of polar coronal plumes [*McComas et al.*, 1995; *Neugebauer et al.*, 1995]. In this study we will present Ulysses solar wind observations from peak southerly latitude on 13 September 1994, across the solar equator and perihelion at 1.34 AU in March 1995, through +64.9° latitude at 1.66 AU on June 7, 1995. Some results from the southbound orbital phase will also be shown to provide proper context for the more recent observations.

OBSERVATIONS

Figure 1 shows six-hour-averaged solar wind speed (upper trace) and density (lower trace, scaled to 1 AU), from peak southerly latitude through +64.9° latitude. The spacecraft encountered continuous fast wind, generally in a range of 700 to 800 km s^{-1}, until -35°, with a slight positive poleward speed gradient. Scaled density was typical of that for high-speed wind, generally within a range of 2.0 to 3.5 cm^{-3}. Structure was evident in both speed and density, but with no obvious periodicity. After a brief excursion below 600 km s^{-1} at -35°, the wind was once again fast until -22°. Simultaneously with its entry into the slow equatorial wind, Ulysses encountered a coronal mass ejection, the first seen since April 1994 [*Gosling et al.*, 1995]. A band of slow-to-medium speed wind spanned -22° through +21° in latitude; faster streams within this band had magnetic polarities corresponding to both the north and south polar coronal holes [*Smith et al.*, 1995]. Stream entry and exit corresponded well with the coronal hole - streamer belt boundaries inferred from observations by the Yohkoh soft X ray telescope and the Mauna Loa K-coronameter. The

streamer belt, which spanned ±60° at the solar surface, had narrowed somewhat by 1.74 solar radii and had narrowed still further, to a total heliographic width of ~43°, at Ulysses (1.4 AU) [*Gosling et al.*, 1995]. The spacecraft reemerged into the high-speed, low density wind near +21°. In the subsequent transit through the northern hemisphere, the average observed speeds and densities appeared to be nearly a mirror image of those seen in the south, with a positive (negative) poleward gradient in speed (density), and speeds consistently above 700 km s^{-1} poleward of +40°.

Table 1 lists solar wind milestones from Ulysses' southward (descending) and northward (ascending) transits through the southern hemisphere, 16 February 1992 through 4 March 1995. Peak speeds, exclusive of CME intervals, were 860 and 856 km s^{-1} during the descending and ascending orbital phases, respectively. The poleward limits of non-CME reverse shocks in the southern hemisphere were farther south than those for forward shocks during both orbital phases, supporting the tilted-CIR model advocated by *Gosling et al.* [1993] and *Pizzo and Gosling* [1994]. The more equatorward locations for both forward and reverse shocks during the ascending orbital phase should be interpreted in the context of a changing Sun and an eccentric orbit. During the southern hemisphere transit, the heliomagnetic current sheet tilt flattened from about 25° to roughly 12° [*Phillips et al.*, 1995*b*]. Furthermore, Ulysses crossed mid and high latitudes southbound at 4 to 2.2 AU, but crossed the same latitudes northbound at 2.2 to 1.4 AU. At the closer heliocentric distances of the ascending phase, the waves bounding CIRs may not yet have steepened into shocks, nor have they propagated as far meridionally.

Latitudinal differences in key solar wind fluid parameters - speed, density, mass flux, and momentum flux - have been determined from *in situ* measurements for the first time over a wide range of latitudes. All parameters are based on mass-weighted protons and alpha particles; parameters involving density have been scaled to 1 AU. Figure 2 shows medians, fifth percentiles, and ninety-fifth percentiles for these properties, sorted by solar rotation, for the out-of-ecliptic mission through June 7, 1995. Note the narrow 5-95% ranges for all parameters poleward

of 40°, and the rough symmetry in all parameters about -80° and about the solar equator. The apparently smooth variation in median wind speed from 10° to 40° results from varying sampling of fast and slow wind, even though the separation between these two wind types was quite distinct. Poleward of 40° a shallow positive poleward speed gradient is evident. Speed was faster at high latitudes, and had a steeper gradient at low latitudes, than for scintillation-based results at a comparable phase of the previous solar cycle [*Rickett and Coles*, 1991]. The 95% level in density is higher near ±20° than at the equator for the ascending orbital phase; this can also be seen in Figure 1, and is probably due to stronger stream interactions away from the equator. Mass flux was much more constant than either speed or density as a result of the general anti-correlation between the latter two quantities. Median mass flux at all latitudes exceeded the values for which the solar wind acceleration could be accounted for by classical thermal conduction, suggesting that extended energy deposition is required [e.g., *Barnes et al.*, 1995].

One unprecedented result visible in Figure 2 is that the momentum flux, equivalent to the pressure exerted by the flowing solar wind, was lower during the northbound transit through low latitudes than at high north or south latitudes. The median values for the rotations centered near -80° and +2° are marked in the lower panel. If one assumes that the local interstellar medium (LISM) is uniform and that its flow vector lies in the solar equatorial plane (it is actually believed to have a 6-8° inclination [*Bertin et al.*, 1993 and references therein]), then the heliopause (HP) in the Sun-centered plane normal to the LISM flow direction should be a constant-pressure surface determined primarily by the solar wind momentum flux. Under the further assumption that momentum flux varies on average as R^{-2}, the HP position should vary with latitude as the square root of the momentum flux at any fixed distance. Figure 3 shows the HP shape based on the median values in Figure 2, normalized by dividing by the equatorial value (1.84 nPa). Measurements since peak southerly latitude, representing solar minimum, are plotted as heavy diamonds; prior Ulysses measurements from the descending orbital phase are shown as open circles. The solid trace is a semicircle, fitted by eye to the more recent data. The measurements suggest that the HP shape

should be circular at higher latitudes but pinched in at the equator, like a figure-eight. This analysis is admittedly oversimplified, neglecting a variety of factors which may influence HP shape, but it illustrates a substantial HP asymmetry which should be considered by modelers.

Previous in-ecliptic results, exploiting the solar dipole tilt to explore a ±25° range of heliomagnetic latitude with Helios and IMP-8 observations, indicated that the total energy flux lost by the Sun via the solar wind was nearly constant with heliomagnetic latitude [e.g., *Bruno et al.*, 1986]. Figure 4 shows the median Ulysses values as functions of heliographic latitude for the plasma-based components of the solar wind energy flux density: gravitational, kinetic, ion and electron enthalpy, electron radial heat flux, and their total. Density was scaled to 1 AU as R^{-2} and electron heat flux was scaled as R^{-3} [*Scime et al.*, 1994]. Ion and electron temperatures were both scaled non-adiabatically as $R^{-0.7}$, roughly in accordance with most empirical determinations. Magnetic and Alfvénic energy fluxes, which we expect to be comparable to or lower than the enthalpy values, were not calculated. The ion heat flux is not included, as it is consistently much lower than the electron heat flux and does not have a well-determined scaling law. The total energy flux density was dominated by the kinetic and gravitational terms and was clearly lower at the equator than at the poles; inclusion of the magnetic and Alfvénic terms would be insufficient to erase this trend. To extend this analysis back to the Sun one needs to incorporate the meridional expansion of the flows from the polar coronal holes, which should increase the deficit in energy flux density from the Sun at low latitudes. The variation in energy flux density with latitude is a previously unrecognized trend; *Bruno et al* [1986] found no significant variation over a ±25° heliomagnetic range. The reasons for the discrepancy between the present study and the Helios/IMP study are unclear, though it may be significant that the Ulysses results represent the declining phase of the solar cycle, whereas the *Bruno et al.* results are from the rising phase. The new findings constitute a significant feature in the solar wind boundary conditions, one that should be considered in theoretical treatments of the solar wind expansion.

SUMMARY

The Ulysses solar wind plasma experiment has returned, and continues to return, a comprehensive set of solar wind proton, alpha particle, and electron measurements throughout the out-of-ecliptic mission. During the ascending orbital phase, Ulysses encountered fast wind except for an equatorial band ~43° wide, demonstrating the limited perspective allowed by in-ecliptic measurements. Speed and density had noticeable poleward gradients even at higher latitudes, with highest speeds and lowest densities near the south pole. The highest non-CME-related wind speed measured to date was 860 km s^{-1}. Although corotating structure was absent from roughly -60° descending to -40° ascending [*Phillips et al.*, 1995*b*], a great deal of structure on shorter time scales was evident in the high-latitude wind. The latitudes of forward and reverse shocks showed the effects of evolution toward the solar minimum configuration, but generally supported the Pizzo-Gosling tilted-CIR model. Mass flux was nearly constant with latitude, at levels suggesting a need for extended deposition of energy [*Barnes et al.*, 1995]. Momentum flux was 37% lower at the equator than at higher latitudes, suggesting a heliopause cross section which is pinched at the equator. Ulysses observations showed that the total solar wind energy flux density at the equator was only about two-thirds of the south polar value. The remainder of the northern hemisphere transit, most of which will occur during solar minimum conditions, will allow further assessment of these trends.

Acknowledgments. We thank R. K. Sakurai and S. J. Kedge for data processing support, and R.J. Forsyth for corroboration of Ulysses events with magnetometer data. Work at Los Alamos was carried out under the auspices of the U.S. Department of Energy with support from NASA.

REFERENCES

Bame, S. J., et al., The Ulysses solar wind plasma experiment, *Astron. Astrophys. Supp. Ser. 92*, 237, 1992.

Bame, S. J., et al., Ulysses observations of a recurrent high speed solar wind stream and the heliomagnetic streamer belt, *Geophys. Res. Lett.*, *20*, 2323, 1993.

Barnes, A., P.R. Gazis, and J.L. Phillips, Constraints on solar wind acceleration mechanisms from Ulysses plasma observations: The first polar pass, *Geophys.Res.Lett.*, in press, 1995.

Bertin, P., et al., Detection of the local interstellar cloud from high-resolution spectroscopy of nearby stars: Inferences on the heliospheric interface, *J. Geophys. Res.*, 98, *15*, 15,193, 1993.

Bruno, R., et al., In-situ observations of the latitudinal gradients of the solar wind parameters during 1976 and 1977, *Solar Phys.*, *104*, 431, 1986.

Gosling, J. T., et al., Latitudinal variation of solar wind corotating stream interaction regions, *Geophys. Res. Lett.*, *20*, 2789, 1993.

Gosling, J. T., et al., A new class of forward-reverse shock pairs in the solar wind, *Geophys. Res. Lett.*, *21*, 2271, 1994.

Gosling, J. T., et al., The band of solar wind variability at low heliographic latitudes near solar activity minimum: Plasma results from the Ulysses rapid latitude scan, *Geophys.Res.Lett.*, in press, 1995.

McComas, D. J., et al., Structures in the polar solar wind: plasma and field observations from Ulysses, *J. Geophys. Res.*, in press, 1995.

Neugebauer, M., et al., Ulysses observations of microstreams in the solar wind from coronal holes, *J. Geophys. Res.*, in press, 1995.

Phillips, J. L., et al., Ulysses solar wind plasma observations at high southerly latitudes, *Science*, *268*, 1030, 1995*a*.

Phillips, J.L., et al., Sources of shocks and compressions in the high-latitude solar wind: Ulysses, *Geophys. Res. Lett.*, in press, 1995*b*.

Pizzo, V. J., and J.T. Gosling, 3-D simulation of high-latitude interaction regions: Comparison with Ulysses results, *Geophys. Res. Lett., 18*, 2063, 1994.

Rickett, B.J., and W.A. Coles, Evolution of the solar wind structure over a solar cycle: Interplanetary scintillation velocity measurements compared with coronal observations, *J. Geophys. Res., 96*, 1717, 1991.

Scime, E.E., et al., Regulation of the solar wind electron heat flux from 1 to 5 AU: Ulysses observations, *J. Geophys. Res., 99*, 23,401, 1994.

Smith, E.J., et al., Results of the Ulysses fast latitude scan: Magnetic field observations, *Geophys. Res. Lett.*, in press, 1995.

Table 1. Solar wind milestones for the Ulysses southern hemisphere transit, in time order. CMEs and adjacent shocked intervals have been deleted in determining highest wind speeds.

Event	Date	Heliocentric distance (AU)	Heliographic latitude (deg.)
Descending (southbound)			
Last slow wind ($V < 450$ km s^{-1})	Apr. 6, 1993	4.84	-28.3
Last non-CME-driven forward shock	Jun. 29, 1993	4.58	-33.6
Last medium wind ($V < 600$ km s^{-1})	Jul. 25, 1993	4.49	-35.4
Last non-CME-driven reverse shock	Apr. 3, 1994	3.34	-58.2
Last coronal mass ejection	Apr. 21-22, 1994	3.24	-60.4 to -60.5
Highest wind speed (860 km s^{-1})	Jul. 4, 1994	2.78	-71.2
Ascending (northbound)			
Highest wind speed (856 km s^{-1})	Dec. 8, 1994	1.70	-56.5
First non-CME-driven reverse shock	Jan. 15, 1995	1.49	-36.1
First medium wind ($V < 600$ km s^{-1})	Jan. 16, 1995	1.48	-35.0
First coronal mass ejection	Feb. 3-5, 1995	1.40	-22.5 to -20.7
First slow wind ($V < 450$ km s^{-1})	Feb. 9, 1995	1.38	-17.9
First non-CME-driven forward shock	Feb. 10, 1995	1.38	-16.9

FIGURE CAPTIONS

Fig. 1. Six-hour averaged solar wind proton flow speed (top trace) and density, scaled to 1 AU (bottom trace) for the ascending orbital phase through June 7, 1995. Heliocentric distance and heliographic latitude are marked at top and bottom, respectively. Crossings of the solar equatorial and ecliptic planes are marked with vertical traces.

Fig. 2. Median, 5%, and 95% values for solar wind fluid parameters, binned by solar rotation and plotted versus heliographic latitude for post-Jupiter observations.

Fig. 3. Postulated shape of the heliopause cross section in a Sun-centered plane normal to the LISM flow vector. Radial distances are based on the square root of 1 AU solar wind momentum flux, divided by the equatorial value. Solid diamonds (open circles) show data before (after) peak southerly latitude. The solid trace is a semicircle, fitted to the diamonds.

Fig. 4. Plasma-based components of the solar wind energy flux density, and their total, versus heliographic latitude. Data were binned by solar rotation. Gaps in electron heat flux represent intervals when sunlight entering the electron spectrometer created a spurious signal; no heat flux value was added to the total flux density for those intervals.

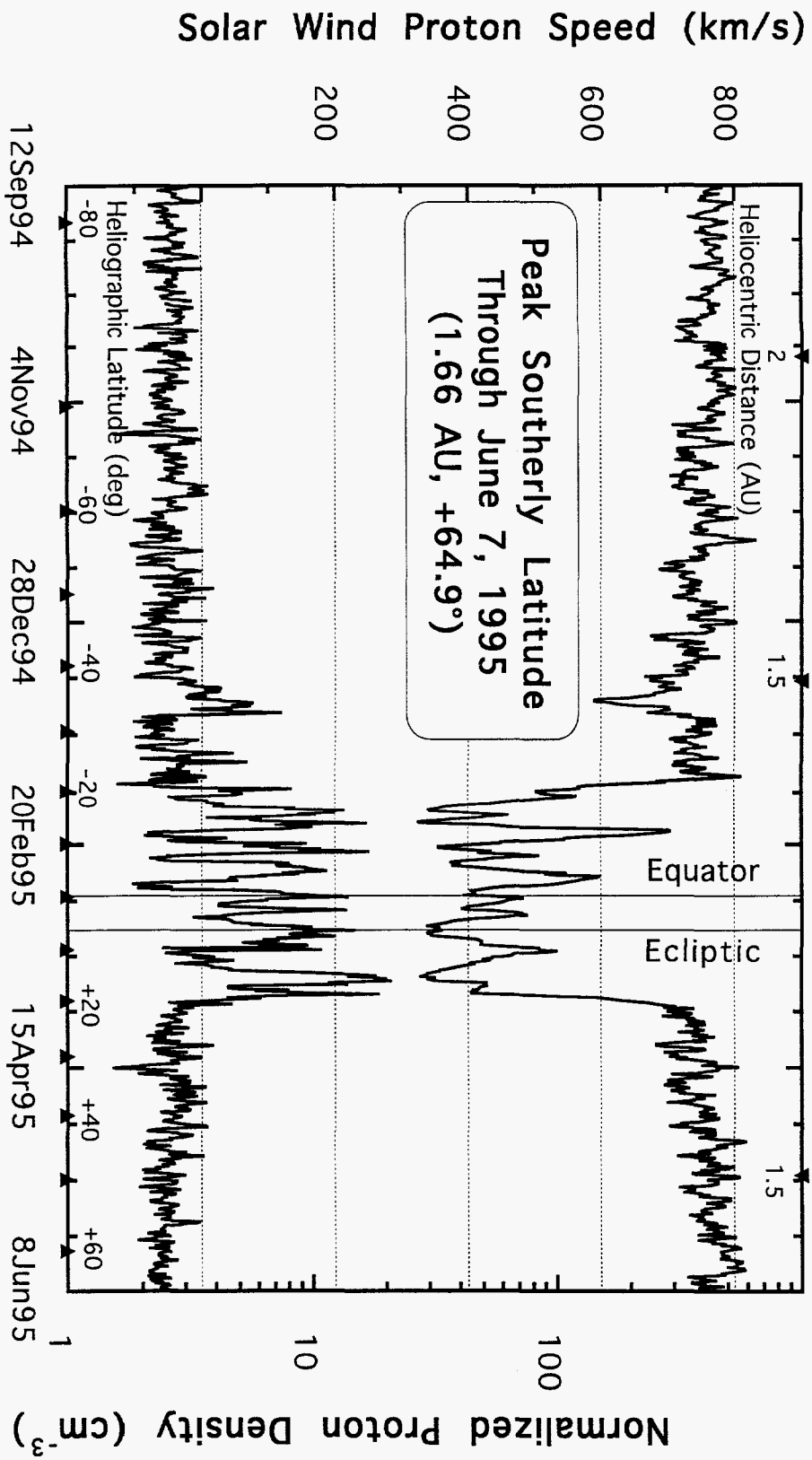
Solar Wind Proton Speed (km/s)
800
600
400
200
Heliocentric Distance (AU)
2
1.5
1.5
Peak Southerly Latitude
Through June 7, 1995
(1.66 AU, +64.9°)
Equator
Ecliptic
Heliographic Latitude (deg)
-80
-60
-40
-20
+20
+40
+60
12Sep94
4Nov94
28Dec94
20Feb95
15Apr95
8Jun95
Normalized Proton Density (cm-3)
100
10
1

FIG. 1

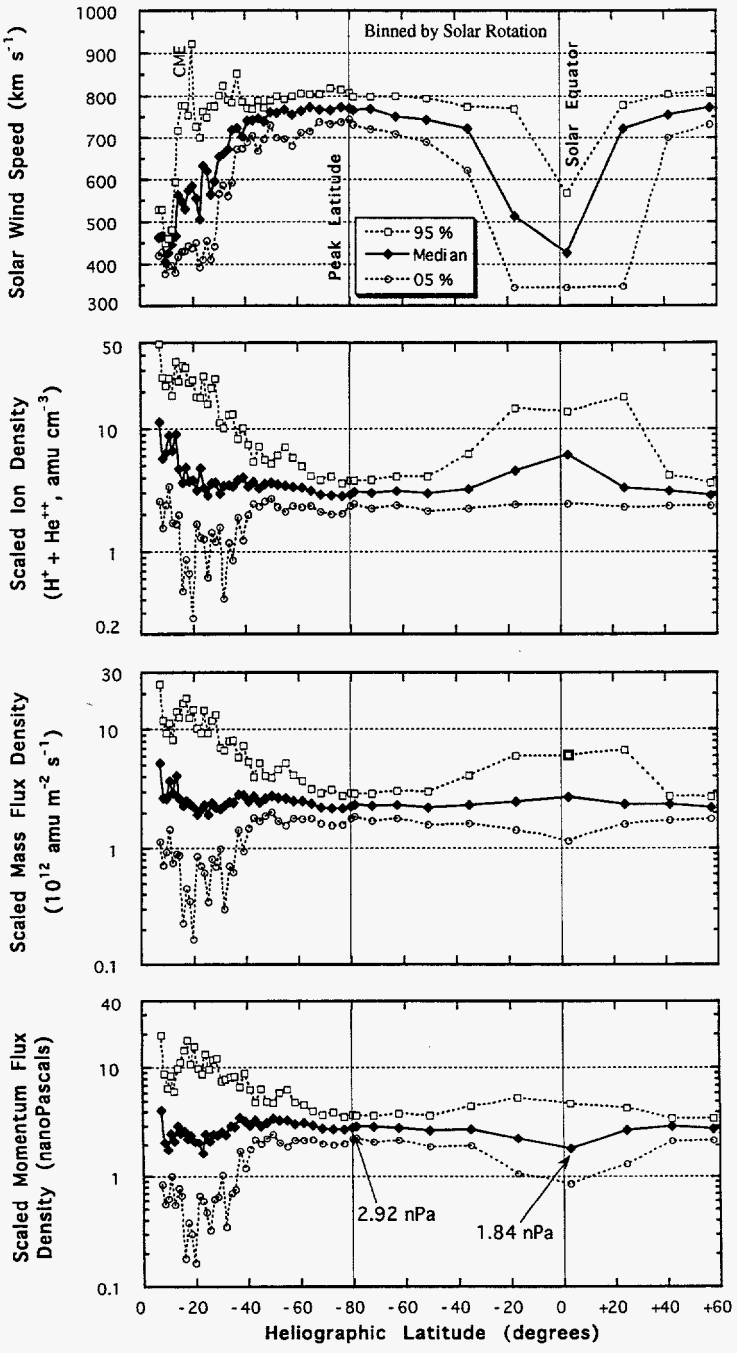
Binned by Solar Rotation
CME
Peak Latitude
Solar Equator
95 %
Median
05 %
Solar Wind Speed (km s^{-1})
Scaled Ion Density ($H^+ + He^{++}$, amu cm^{-3})
Scaled Mass Flux Density (10^{12} amu m^{-2} s^{-1})
Scaled Momentum Flux Density (nanoPascals)
2.92 nPa
1.84 nPa
Heliographic Latitude (degrees)

FIG. 2

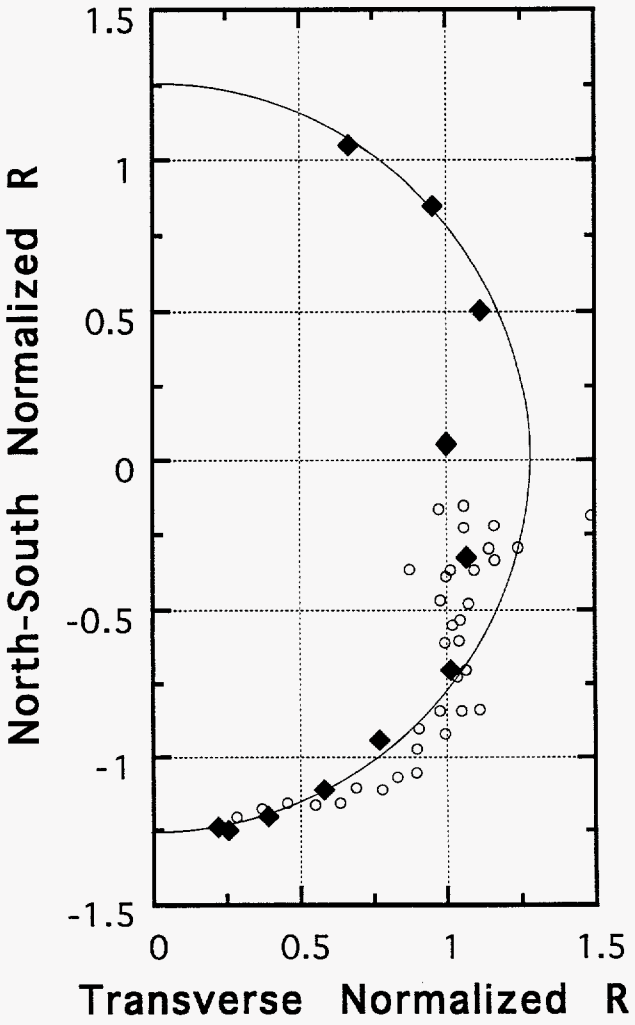
1.5
1
0.5
0
-0.5
-1
-1.5
0
0.5
1
1.5
North-South Normalized R
Transverse Normalized R

FIG. 3

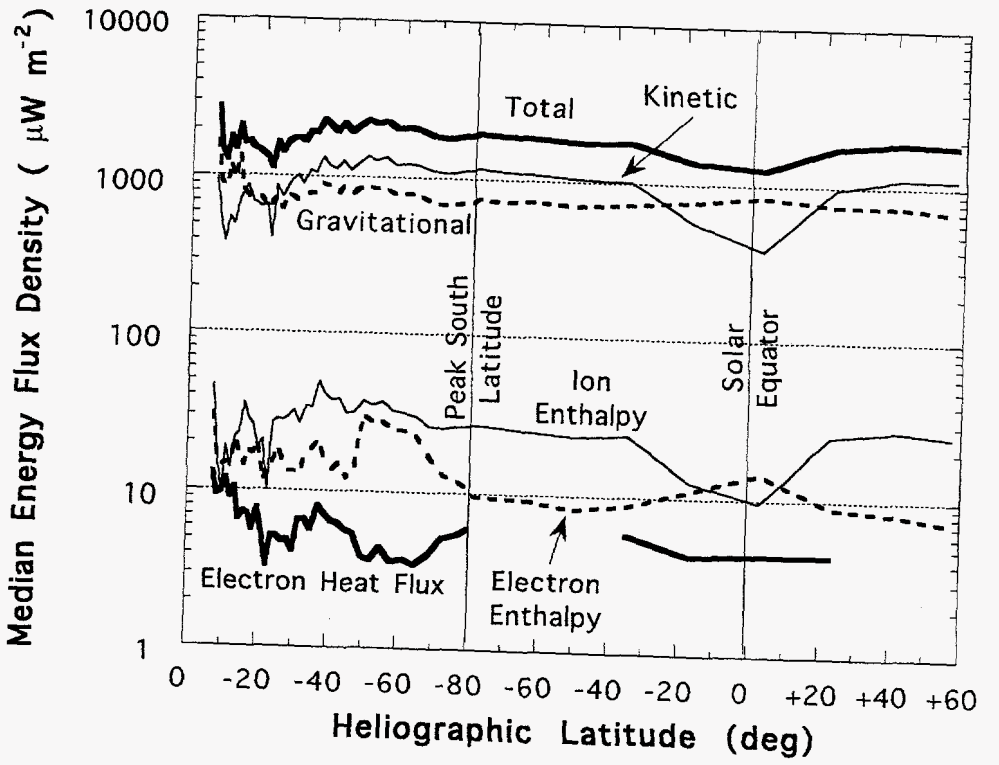

DISCLAIMER

FIG. 4